The McGraw-Hill Companies

Education

1

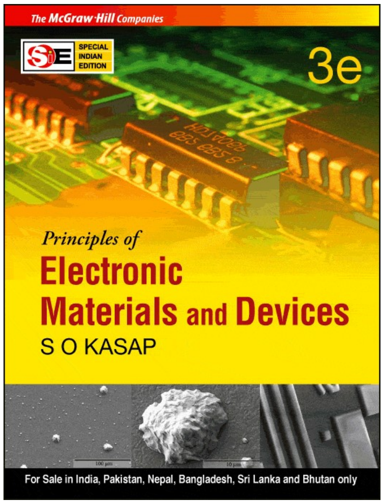

Chapter 6

Semiconductor Devices

1

Properties of pn junction

2

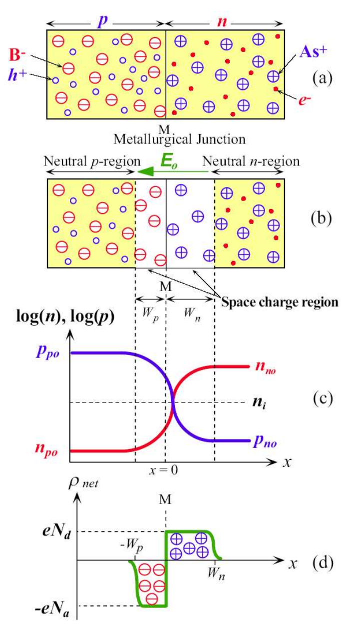

Assumption:

$N_d < N_a$

2

3

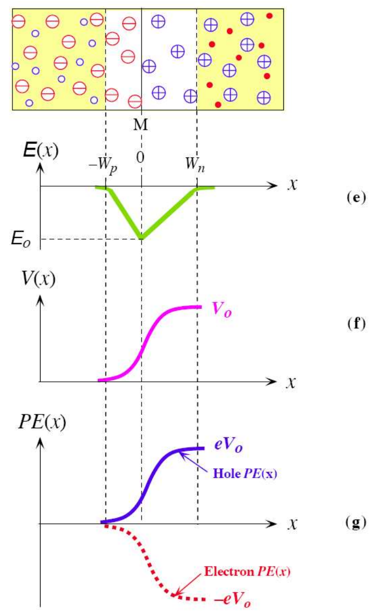

3

4

Ideal *pn* Junction

Acceptor concentration Donor concentration

Depletion Widths

$$N_a W_p = N_d W_n$$

Field (*E*) and net space charge density

Net space charge density

$$\frac{d\mathcal{E}}{dx} = \frac{\rho_{\text{net}}(x)}{\varepsilon}$$

Permittivity of the medium

Field in depletion region

$$\mathcal{E}(x) = \frac{1}{\varepsilon}\int_{-W_p}^{x} \rho_{\text{net}}(x)dx$$

Electric Field

4

5

Ideal *pn* Junction

Built-in field

$$\mathcal{E}_o = -\frac{eN_d W_n}{\varepsilon}$$

where $\varepsilon = \varepsilon_o\, \varepsilon_r$

Built-in voltage

$$V_o = \frac{kT}{e}\ln\left(\frac{N_a N_d}{n_i^2}\right)$$

where n_i is the intrinsic concentration

Depletion region width

$$W_o = \left[\frac{2\varepsilon\left(N_a + N_d\right)V_o}{eN_a N_d}\right]^{1/2}$$

where $W_o = W_n + W_p$ is the total width of the depletion region under a zero applied voltage

5

Forward Bias

6

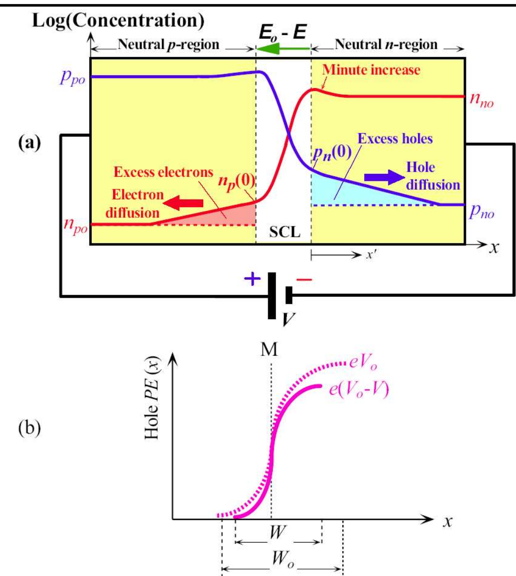

Forward biased *pn* junction and the injection of minority carriers.
(a) Carrier concentration profiles across the device under forward bias.
(b) The hole potential energy with and without an applied bias. W is the width of the SCL with forward bias.

6

Forward Bias: Diffusion Current

Law of the Junction: Minority Carrier Concentrations and Voltage

$$p_n(0) = p_{no} \exp\left(\frac{eV}{kT}\right)$$

$$n_p(0) = n_{po} \exp\left(\frac{eV}{kT}\right)$$

$p_n(0)$ is the hole concentration just outside the depletion region on the *n*-side

$n_p(0)$ is the electron concentration just outside the depletion region on the *p*-side

Forward Bias: Diffusion Current

Excess minority carrier concentration profile

$$\Delta p_n(x') = \Delta p_n(0) \exp\left(-\frac{x'}{L_h}\right)$$

where L_h is the hole diffusion length, defined by $L_h = \sqrt{D_h \tau_h}$ in which τ_h is the mean hole recombination lifetime (minority carrier lifetime in the *n*-region.

Excess minority carrier concentration

$$\Delta p_n(x') = p_n(x') - p_{no}$$

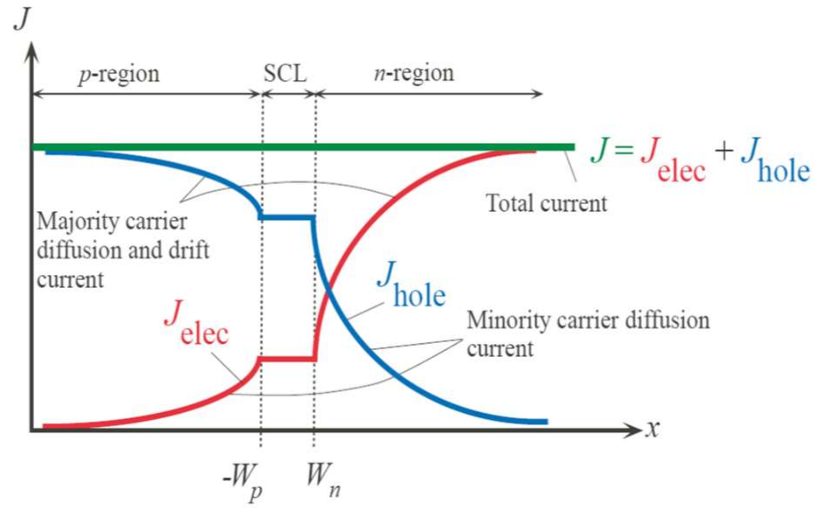

The total current anywhere in the device is constant. Just outside the depletion region it is due to the diffusion of minority carriers.

9

Forward Bias: Diffusion Current

Hole diffusion current in *n*-side in the neutral region

$$J_{D,\text{hole}} = \left(\frac{eD_h n_i^2}{L_h N_d}\right)\left[\exp\left(\frac{eV}{kT}-1\right)\right]$$

There is a similar expression for the electron diffusion current density $J_{D,\text{elec}}$ in the *p*-region.

10

Forward Bias: Diffusion Current

Ideal diode (Shockley) equation

$$J = J_{so}\left[\exp\left(\frac{eV}{kT}\right) - 1\right]$$

Reverse saturation current density

$$J_{so} = \left[\left(\frac{eD_h}{L_h N_d}\right) + \left(\frac{eD_e}{L_e N_a}\right)\right] n_i^2$$

11

Forward Bias: Diffusion Current

Intrinsic concentration

$$n_i^2 = (N_c N_v)\exp\left(-\frac{eV_g}{kT}\right)$$

where $V_g = E_g / e$ is the bandgap energy expressed in volts

$V_g =$ 0.67 V for Ge, 1.1 V for Si, and 1.42 V for GaAs

$$J = J_{so}\exp\left(\frac{eV}{kT}\right) = C\exp\left(\frac{e(V - V_g)}{kT}\right) \qquad V > kT/e$$

We can plot I vs. V for Ge, Si and Ge

12

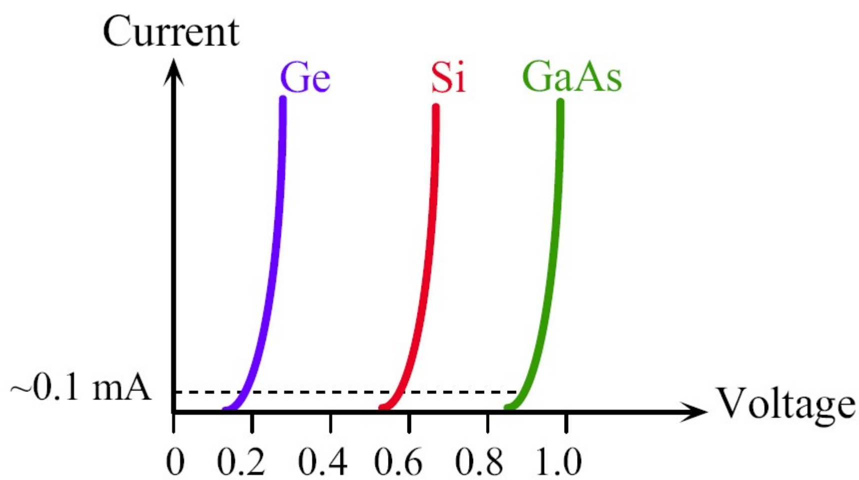

Schematic sketch of the I-V characteristics of Ge, Si, and GaAs pn junctions.

13

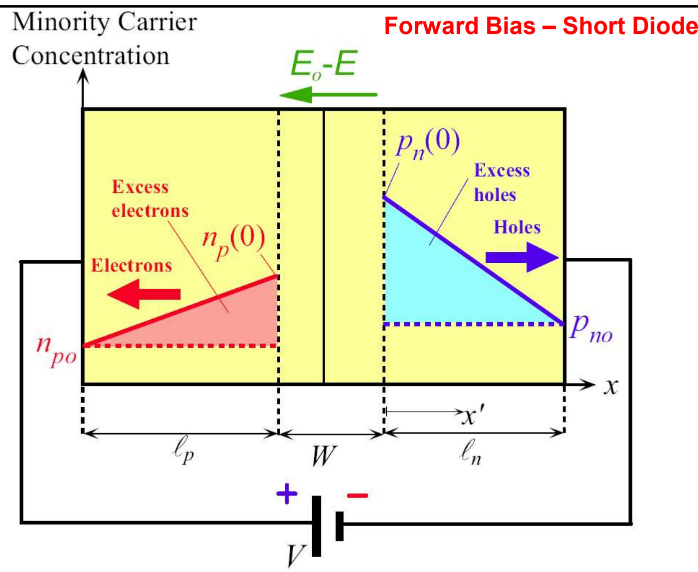

Minority carrier injection and diffusion in a short diode.

14

15

Forward Bias: Diffusion Current

Short Diode

$$J = \left(\frac{eD_h}{\ell_n N_d} + \frac{eD_e}{\ell_p N_a} \right) n_i^2 \left[\exp\left(\frac{eV}{kT} \right) - 1 \right]$$

where ℓ_n and ℓ_p represent the lengths of the neutral *n*- and *p*-regions outside the depletion region.

15

16

Forward Bias: Recombination Current

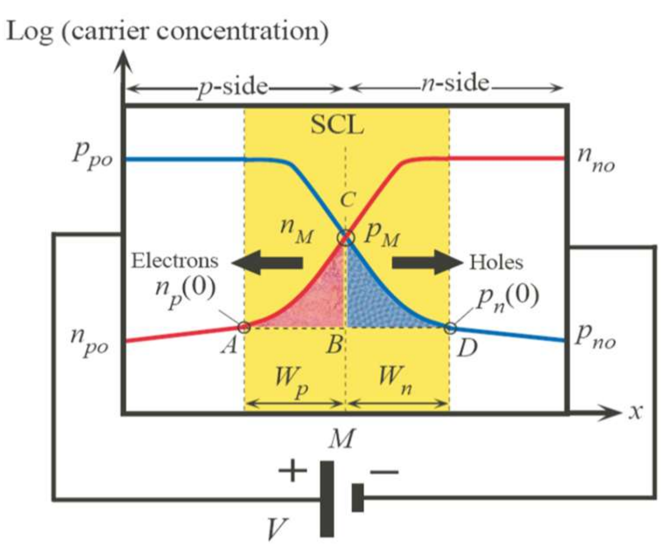

Forward biased pn junction and the injection of carriers and their recombination in the SCL

16

Forward Bias: Recombination and Total Current

17

Recombination Current

$$J_{\text{recom}} = J_{ro}[\exp(eV/2kT) - 1] \quad \text{where } J_{ro} = \frac{en_i}{2}\left(\frac{W_p}{\tau_e} + \frac{W_n}{\tau_h}\right)$$

Total diode current = diffusion + recombination

$$J = J_{so}\exp\left(\frac{eV}{kT}\right) + J_{ro}\exp\left(\frac{eV}{2kT}\right) \qquad V > \frac{kT}{e}$$

The diode equation

$$J = J_o \exp\left(\frac{eV}{\eta kT}\right) \qquad V > \frac{kT}{e}$$

Where J_o is a new constant and η is an ideality factor

17

18

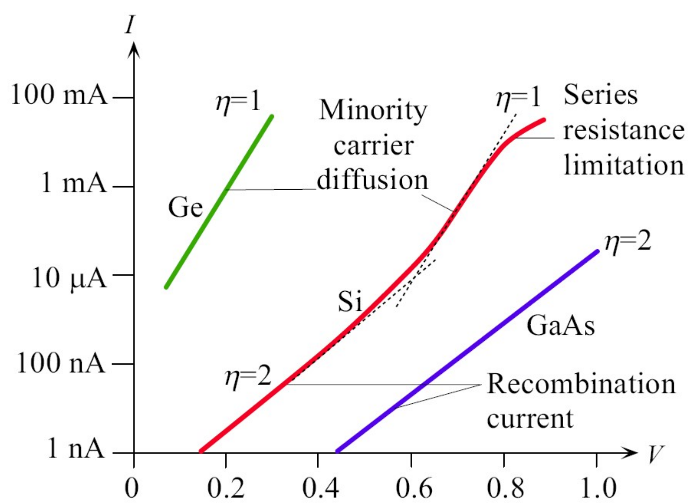

Schematic sketch of typical *I-V* characteristics of Ge, Si and GaAs pn junctions as log(*I*) vs. *V*. The slope indicates $e/(\eta kT)$

18

19

Reverse Bias: pn junction

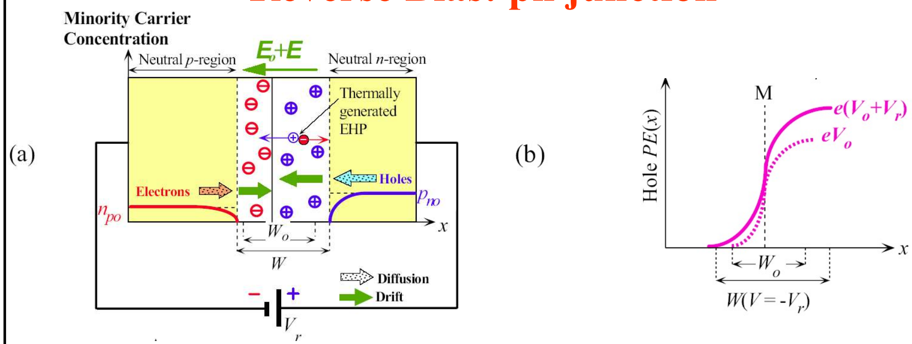

Reverse biased pn junction. (a) Minority carrier profiles and the origin of the reverse current. (b) Hole PE across the junction under reverse bias

$$J_{rev} = \left[\left(\frac{eD_h}{L_hN_d}\right)+\left(\frac{eD_e}{L_eN_a}\right)\right]n_i^2 + \frac{eWn_i}{\tau_g}$$

19

20

Reverse Bias

Total Reverse Current

$$J_{\text{rev}} = \underbrace{\left(\frac{eD_h}{L_hN_d}+\frac{eD_e}{L_eN_a}\right)n_i^2}_{\substack{\text{Diffusion current in neutral regions}\\ \text{the Shockley reverse current}}} + \overbrace{\frac{eWn_i}{\tau_g}}^{\text{Thermal generation in depletion region}}$$

Mean thermal generation time

20

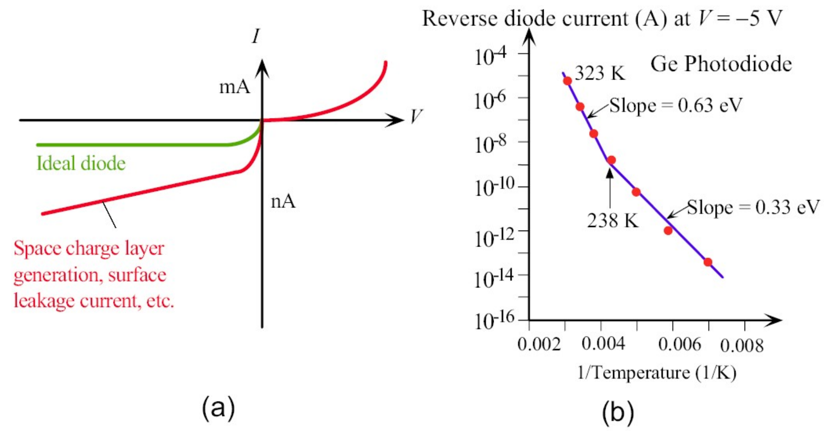

(a) Reverse I-V characteristics of a pn junction (the positive and negative current axes have different scales). (b) Reverse diode current in a Ge pn junction as a function of temperature in a $\ln(I_{rev})$ vs $1/T$ plot. Above 238 K, I_{rev} is controlled by n_i^2 and below 238 K it is controlled by n_i. The vertical axis is a logarithmic scale with actual current values. (From D. Scansen and S.O. Kasap, *Cnd. J. Physics*. **70**, 1070-1075, 1992.)

pn Junction: Band Diagram

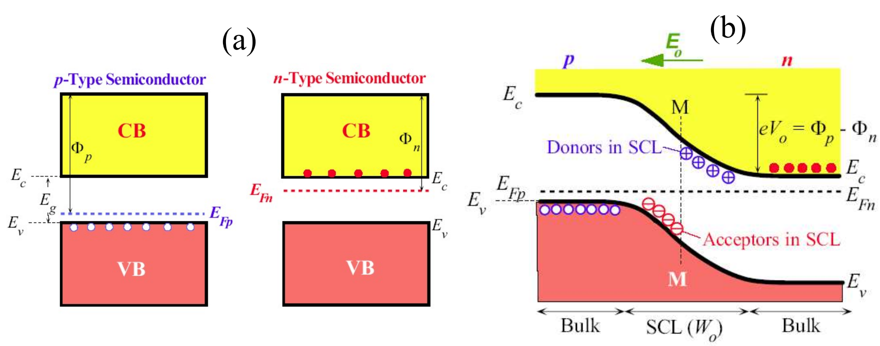

(a) Two isolated *p* and *n*-type semiconductors (same material).
(b) A pn junction band diagram when the two semiconductors are in contact. The Fermi level must be uniform in equilibrium. The metallurgical junction is at M. The region around M contains the space charge layer (SCL). On the *n*-side of M, SCL has the exposed positively charged donors whereas on the p-side it has the exposed negatively charged acceptors.

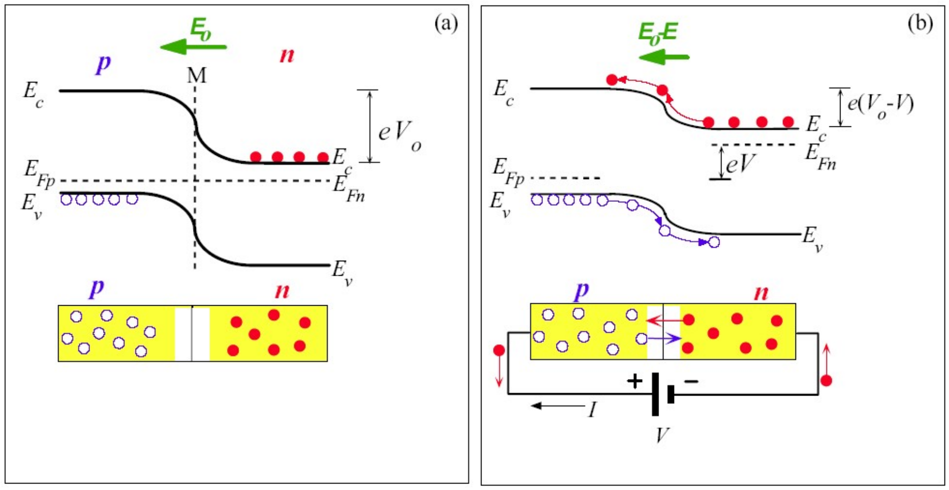

Energy band diagrams for a pn junction under
(a) open circuit and
(b) forward bias

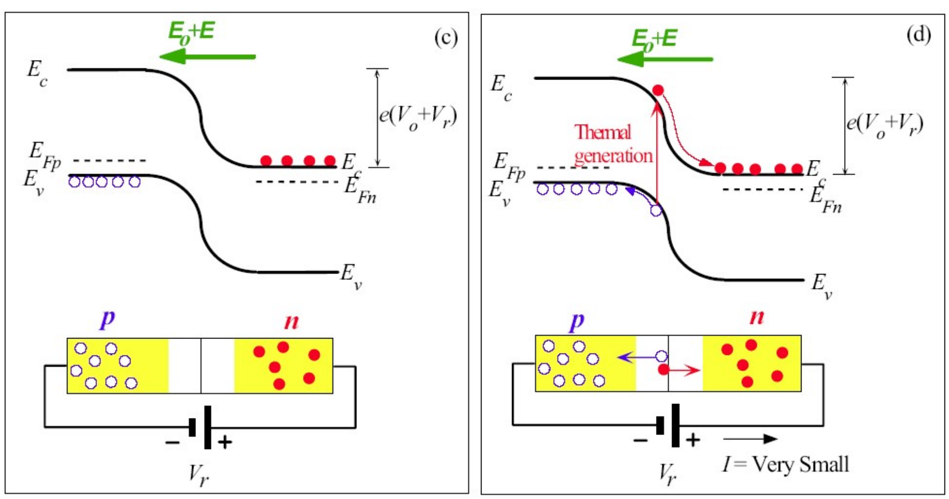

Energy band diagrams for a pn junction under
(c) reverse bias conditions.
(d) Thermal generation of electron hole pairs in the depletion region results in a small reverse current.

Depletion Capacitance

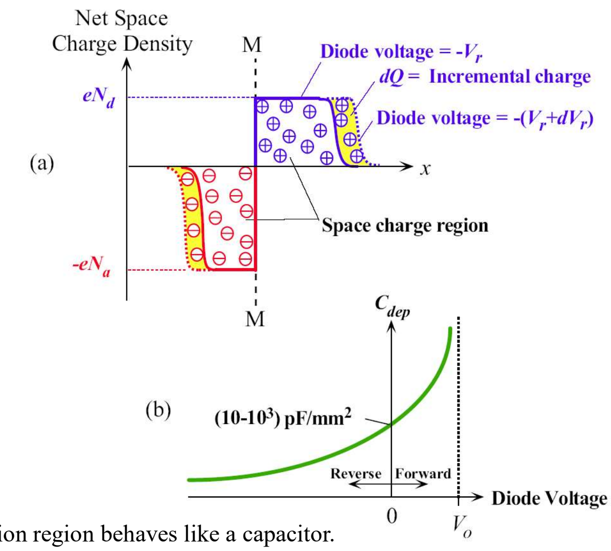

The depletion region behaves like a capacitor.

(a) The charge in the depletion region depends on the applied voltage just as in a capacitor

(b) The incremental capacitances of the depletion region increases with forward bias and decreases with reverse bias. Its value is typically in the range of picofarads per mm^2

Depletion layer capacitance of the pn junction

Depletion region width

$$W = \left[\frac{2\varepsilon(N_a + N_d)(V_o - V)}{eN_aN_d}\right]^{1/2}$$

where, for forward bias, V is positive, which reduces V_o, and, for reverse bias, V is negative , so V_o is increased.

Definition of depletion layer capacitance C_{dep}

$$C_{\text{dep}} = \left|\frac{dQ}{dV}\right|$$

where the amount of charge on any one side of the depletion layer is $|Q| = eN_dW_nA = eN_aW_pA$ and $W = W_n + W_p$

Depletion Capacitance

27

$$C_{\text{dep}} = \frac{\varepsilon A}{W} = \frac{A}{(V_o - V)^{1/2}}\left[\frac{e\varepsilon(N_a N_d)}{2(N_a + N_d)}\right]^{1/2}$$

27

Diffusion Capacitance

28

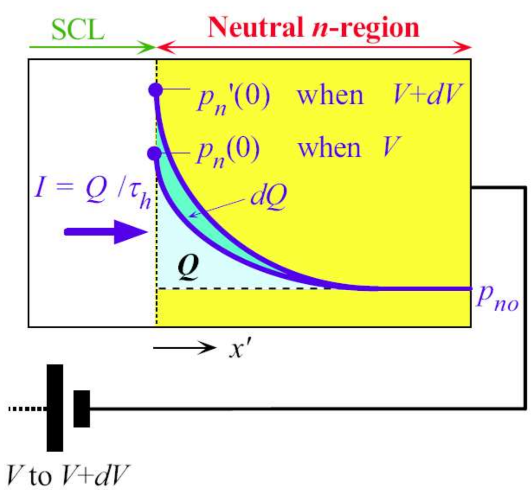

Consider the injection of holes into the *n*-side during forward bias. Storage or diffusion capacitance arises because when the diode voltage increases from V to $V+dV$ then more minority carriers are injected and more minority carrier charge is stored in the *n*-region.

28

Dynamic Resistance

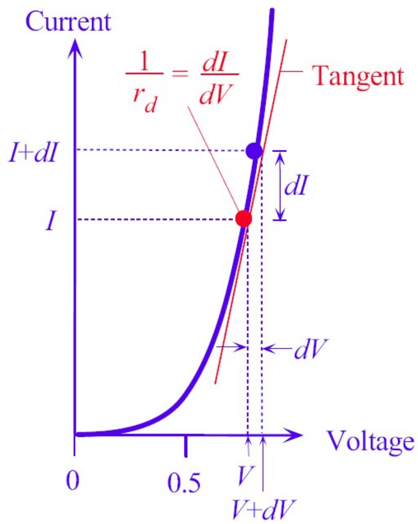

The dynamic resistance of the diode is defined as *dV/dI* which is the inverse of the tangent at *I*.

29

Diffusion capacitance and dynamic resistance

Diffusion capacitance

$$C_{\text{diff}} = \frac{dQ}{dV} = \frac{\tau_h eI}{kT} = \frac{\tau_h I(\text{mA})}{25}$$

where we used $e/kT \approx 40 = 1/0.025$ at room temperature

Dynamic incremental resistance

$$r_d = \frac{dV}{dI} = \frac{kT}{eI} = \frac{25}{I(\text{mA})}$$

30

31

Reverse Breakdown

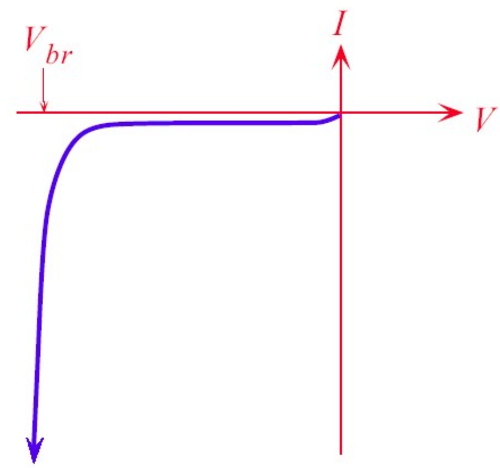

Reverse *I-V* characteristics of a *pn* junction.

31

32

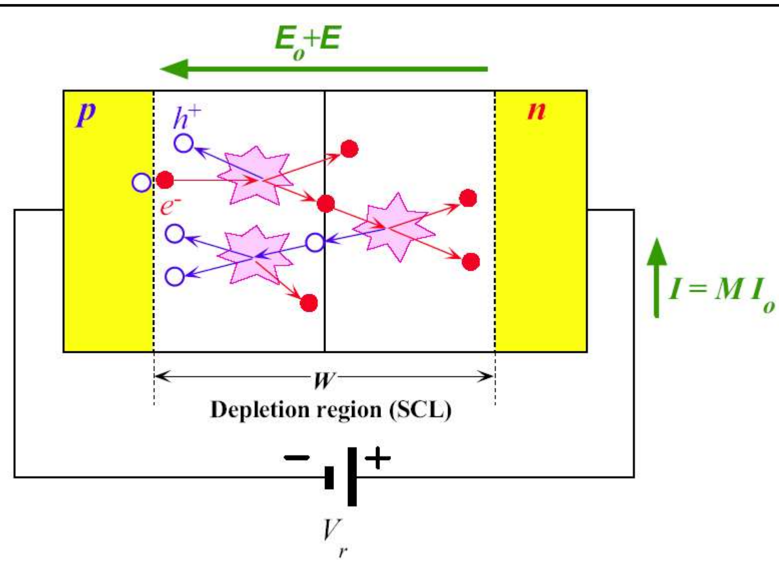

Avalanche breakdown by impact ionization.

32

33

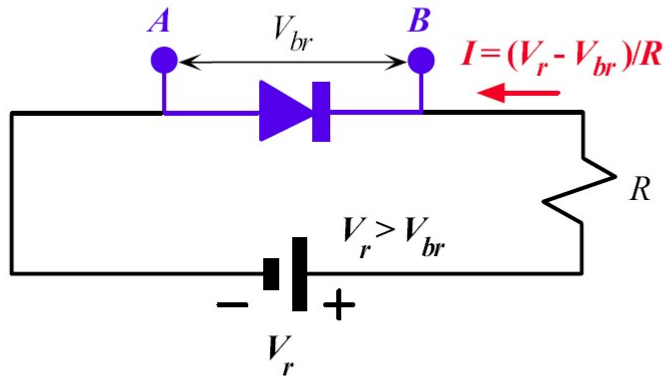

If the reverse breakdown current when $V_r > V_{br}$ is limited by an external resistance, R, to prevent destructive power dissipation then the diode can be used to clamp the voltage between A and B to remain approximately V_{br}.

33

34

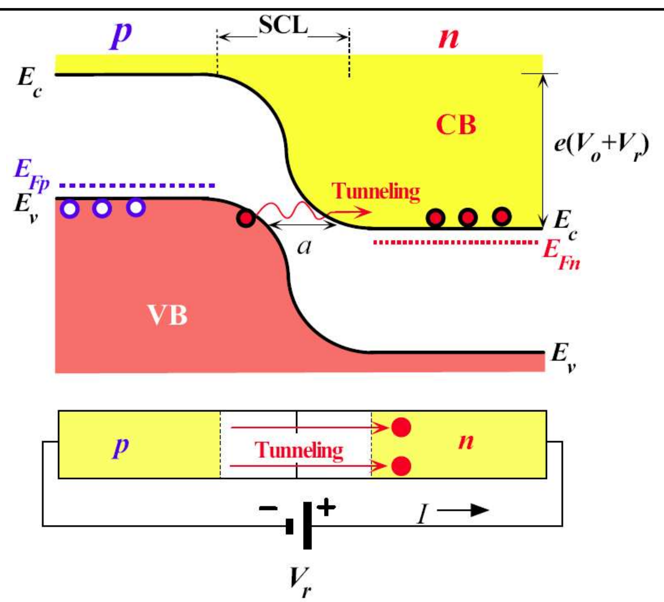

Zener breakdown involves electrons tunneling from the VB of p side to the CB of n-side when the reverse bias reduces E_c to line up with E_v.

34

35

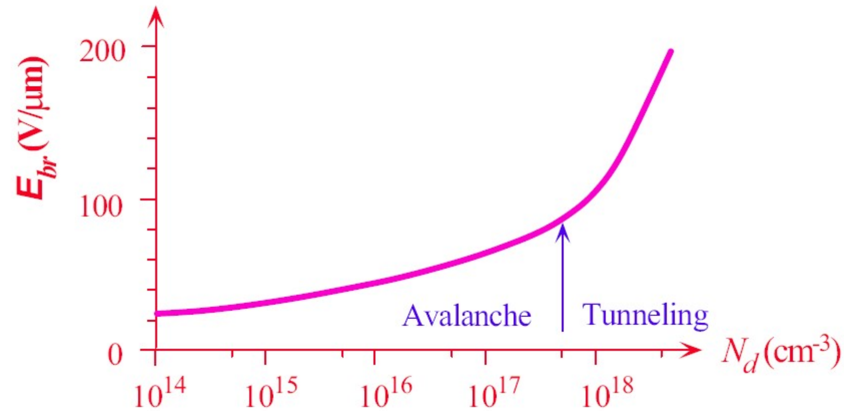

The breakdown field E_{br} in the depletion layer for the onset of reverse breakdown vs. doping concentration N_d in the lightly doped region in a one-sided (p^+n or pn^+) abrupt pn junction. avalanche and tunneling mechanisms are separated by the arrow [data extracted from M.Sze and G. Gibbons, Solid. State. Electronics, 9, 831 (1966)]

35

36

This flash light uses a white **LED** instead of an incandescent light bulb. The flash light can operate continuously for 200 hours and can project an intense spot over 30 feet.

36

Recalling: Recombination

37

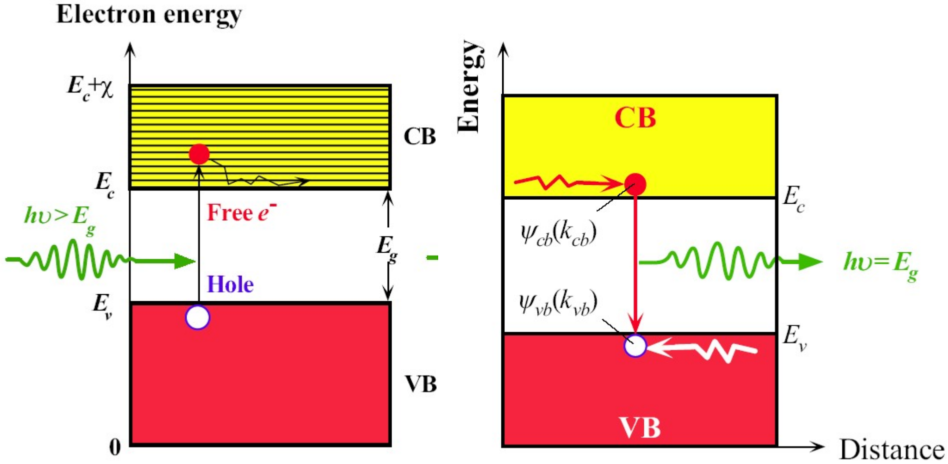

Direct recombination in GaAs.
$k_{cb} = k_{vb}$ so that momentum conservation is satisfied.

37

Recalling: Direct Bandgap Semiconductor

38

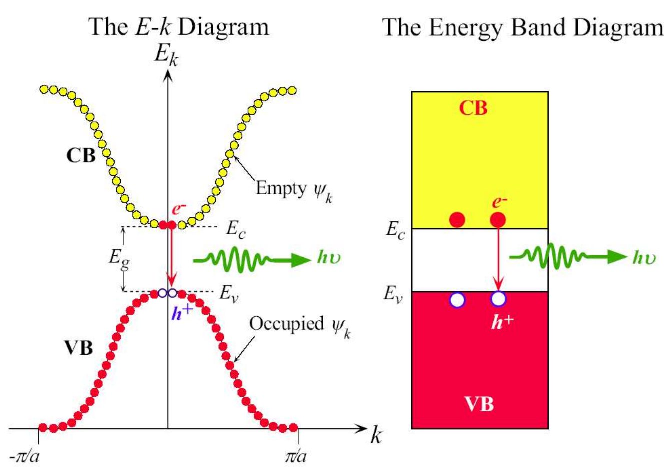

The E-k diagram of a direct bandgap semiconductor such as GaAs. The E-k curve consists of many discrete points each point corresponding to a possible state, wavefunction $\psi_k(x)$ that is allowed to exist in the crystal. The points are so close that we normally draw the E-k relationship as a continuous curve. In the energy range E_v to E_c there are no points ($\psi_k(x)$ solutions).

38

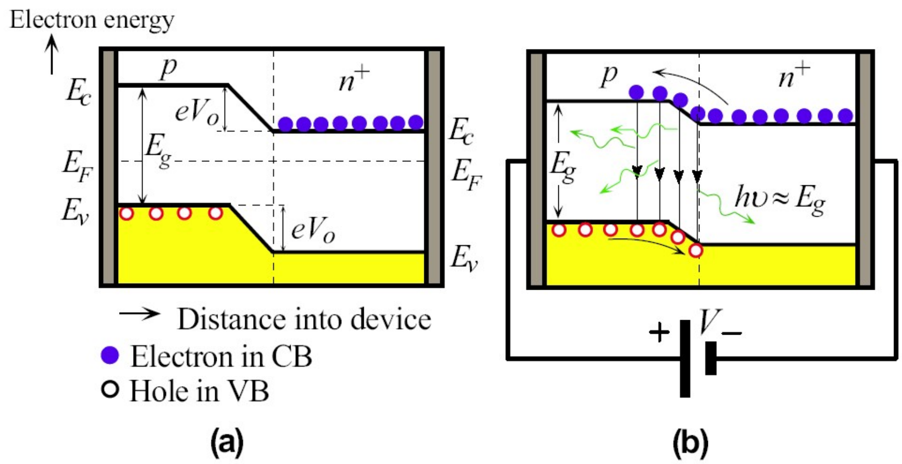

(a) The energy band diagram of a *p*-n^+ (heavily *n*-type doped) junction without any bias. Built-in potential V_0 prevents electrons from diffusing from n^+ to *p* side.
(b) The applied bias reduces V_0 and thereby allows electrons to diffuse, be injected, into the *p*-side. Recombination around the junction and within the diffusion length of the electrons in the *p*-side leads to photon emission.

39

40

Structure of LED

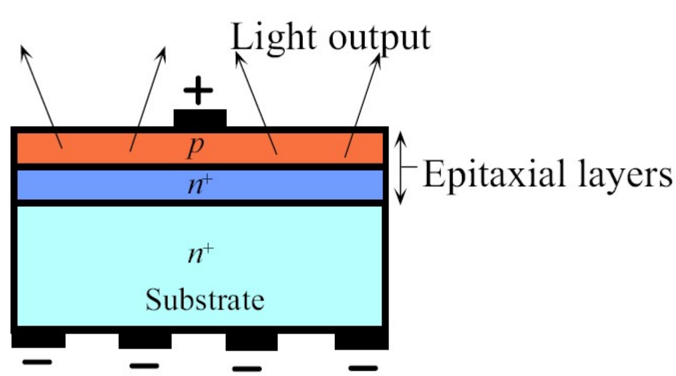

A schematic illustration of one possible LED device structure. First n^+ is epitaxially grown on a substrate. A thin *p* layer is then epitaxially grown on the first layer.

40

Structure of LED: Importance of Lattice Grading

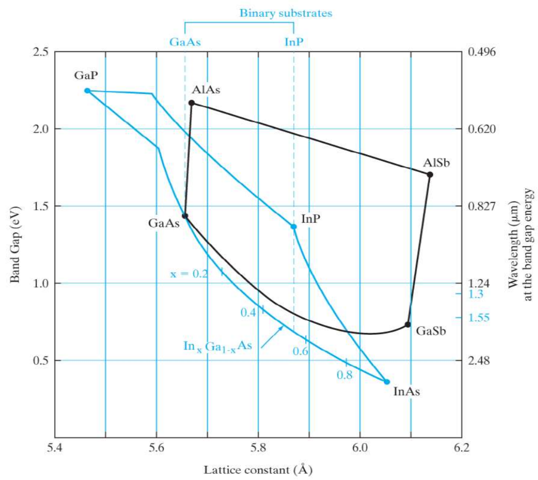

41

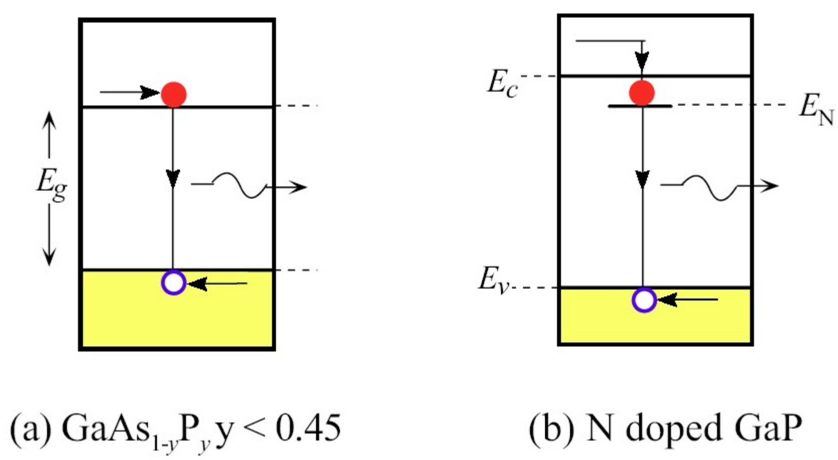

(a) Photon emission in a direct bandgap semiconductor.
(b) GaP is an indirect bandgap semiconductor. When doped with nitrogen there is an electron recombination center at E_N. Direct recombination between a captured electron at E_N and a hole emits a photon.

42

Light Emitting Diodes (LEDs)

External efficiency, η_{external}

$$\eta_{\text{external}} = \frac{P_{\text{out}}(\text{optical})}{IV} \times 100\%$$

43

Table 6.2 Selected LED semiconductor materials

Semiconductor Active Layer	Structure	D or I	λ (nm)	η_{external} (%)	Comments
GaAs	DH	D	870–900	10	Infrared (IR)
$Al_xGa_{1-x}As$ $(0 < x < 0.4)$	DH	D	640–870	3–20	Red to IR
$In_{1-x}Ga_xAs_yP_{1-y}$ $(y \approx 2.20x, 0 < x < 0.47)$	DH	D	1–1.6 μm	>10	LEDs in communications
$In_{0.49}Al_xGa_{0.51-x}P$	DH	D	590–630	>10	Amber, green, red; high luminous intensity
InGaN/GaN quantum well	QW	D	450–530	5–20	Blue to green
$GaAs_{1-y}P_y$ $(y < 0.45)$	HJ	D	630–870	< 1	Red to IR
$GaAs_{1-y}P_y$ $(y > 0.45)$ (N or Zn, O doping)	HJ	I	560–700	< 1	Red, orange, yellow
SiC	HJ	I	460–470	0.02	Blue, low efficiency
GaP (Zn)	HJ	I	700	2–3	Red
GaP (N)	HJ	I	565	< 1	Green

NOTE: Optical communication channels are at 850 nm (local network) and at 1.3 and 1.55 μm (long distance). D = direct bandgap, I = indirect bandgap. η_{external} is typical and may vary substantially depending on the device structure. DH = double heterostructure, HJ = homojunction, QW = quantum well.

44

Double Hetero-Structure LED

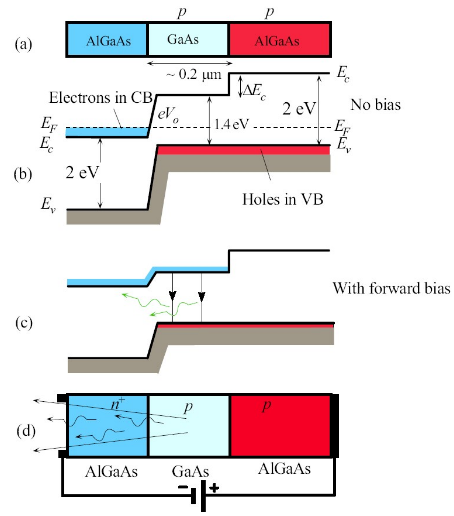

(a) A double heterostructure diode has two junctions which are between two different bandgap semiconductors (GaAs and AlGaAs). (b) A simplified energy band diagram with exaggerated features. EF must be uniform. (c) Forward biased simplified energy band diagram. (d) Forward biased LED. Schematic illustration of photons escaping reabsorption in the AlGaAs layer and being emitted from the device.

45

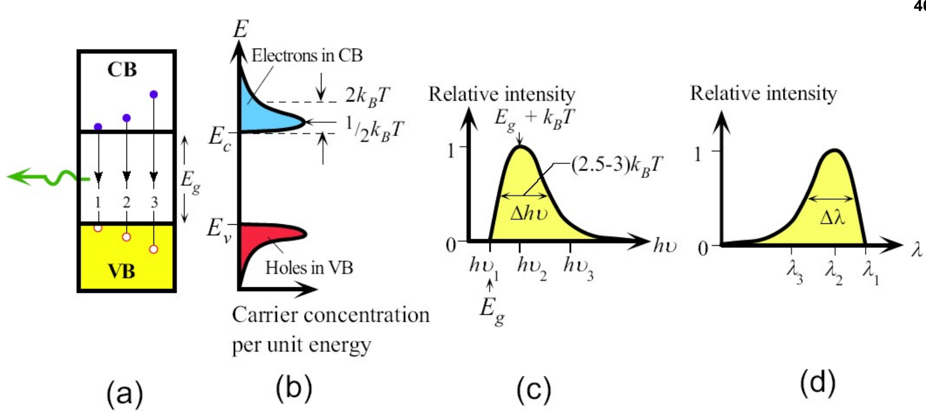

(a) Energy band diagram with possible recombination paths. (b) Energy distribution of electrons in the CB and holes in the VB. The highest electron concentration is (1/2)kT above E_c. (c) The relative light intensity as a function of photon energy based on (b). (d) Relative intensity as a function of wavelength in the output spectrum based on (b) and (c).

46

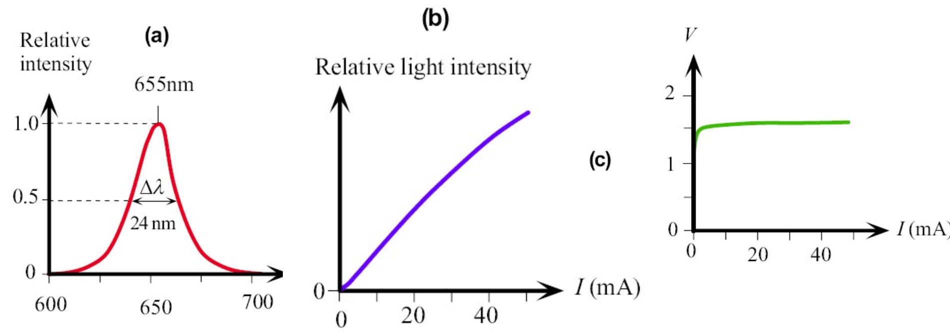

(a) A typical output spectrum (relative intensity vs wavelength) from a red GaAsP LED. (b) Typical output light power vs. forward current. (c) Typical *I-V* characteristics of a red LED. The turn-on voltage is around 1.5V

47

LED Characteristics

Spread in the emitted photon energies, Δ(*hυ*), is

$$\Delta(h\upsilon) \approx 3kT$$

LED spectral linewidth, □□

$$\Delta\lambda = \lambda^2 \frac{3kT}{hc}$$

Example: At room temperature

$$\lambda = 1550\,\text{nm} \longrightarrow \Delta\lambda = 150\,\text{nm}$$

48

Luminescence and Phosphors

49

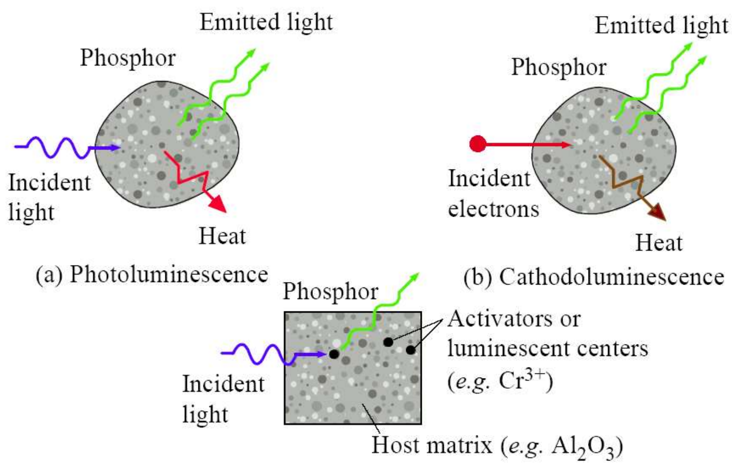

Photoluminescence, cathodoluminescence and a typical phosphor

Photoluminiscence, X-ray luminescence, Cathodoluminiscence, Electroluminiscence, Fluorescence, Phophorescence

49

Photoluminescence

50

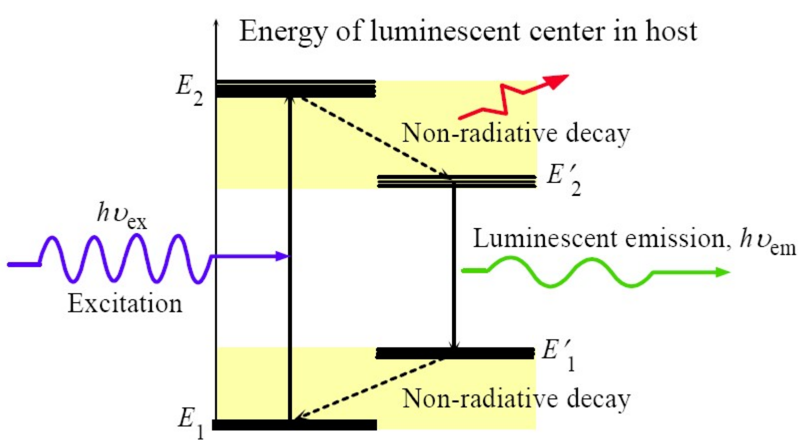

Photoluminescence: light absorption, excitation, nonradiative decay and light emission, and Return to the ground state E_1.
The energy levels have been displaced horizontally for clarity.

50

Luminescent Emission

51

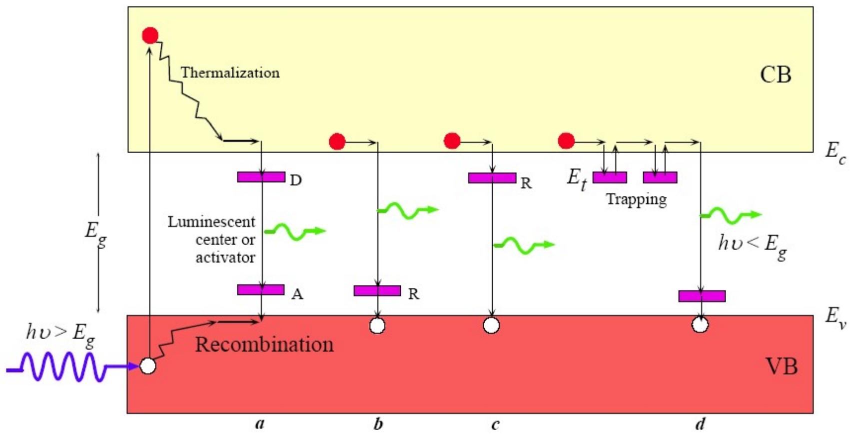

Optical absorption generates an EHP. Both carriers thermalize. There are a number of recombination processes via a dopant that can result in a luminescent emission.

51

White LEDs

52

$Y_3Al_5O_{12}:Ce^{3+}$ (known as "YAG")
cerium doped phosphor coating

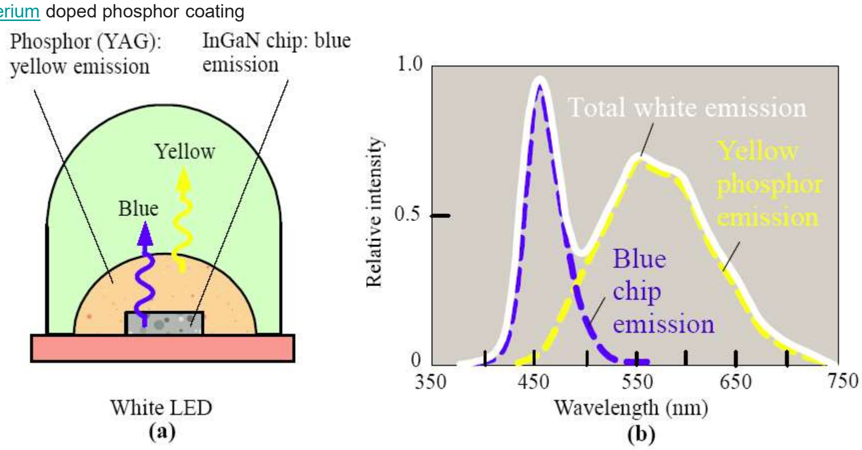

(a) A typical "white" LED structure. (b) The spectral distribution of light emitted by a white LED. Blue luminescence is emitted by the GaInN chip and "yellow" phosphorescence or luminescence is produced by a phosphor. The combined spectrum looks "white".

Isamu Akasaki and Hiroshi Amano, Shuji Nakamura were awarded the Nobel Prize in Physics in 2014 for the invention (back in 1993) of the blue LED.

52

Table 9.4 Selected phosphor examples

Phosphor	Activator	Useful Emission	Example Excitation	Comment or Application
$Y_2O_3:Eu^{3+}$	Eu^{3+}	Red	UV	Fluorescent lamp, color TV
$BaMgAl_{10}O_{17}:Eu^{2+}$	Eu^{2+}	Blue	UV	Fluorescent lamp
$CeMgAl_{11}O_{19}:Tb^{3+}$	Tb^{3+}	Green	UV	Fluorescent lamp
$Y_3Al_5O_{12}:Ce^{3+}$	Ce^{3+}	Yellow	Blue, violet	White LED
$Sr_2SiO_4:Eu^{3+}$	Eu^{3+}	Yellow	Violet	White LED (experimental)
$ZnS:Ag^+$	Ag^+	Blue	Electron beam	Color TV blue phosphor
$Zn_{0.68}Cd_{0.32}S:Ag^+$	Ag^+	Green	Electron beam	Color TV green phosphor
$ZnS:Cu^+$	Cu^+	Green	Electron beam	Color TV green phosphor

This part of Phosphorescence and blue LEDs is available in chapter 9.13 (p-820) of the text book.

53

***pn* Junction Si solar cells at work. Honda's two seated Dream car is powered by photovoltaics. The Honda Dream was first to finish 3,010 km in four days in the 1996 World Solar Challenge.**

|SOURCE: Courtesy of Centre for Photovoltaic Engineering, University of New South Wales, Sydney, Australia.

54

Solar Cells: Photovoltaics

55

NASA Dryden Flight Research Center Photo Collection
http://www.dfrc.nasa.gov/gallery/photo/index.html
NASA Photo: ED01-0209-5 Date: July 14, 2001 Photo by: Nick Galante/PMRF
The Helios Prototype flying wing is shown near the Hawaiian islands of Niihau and Lehua during its first test flight on solar power from the U.S. Navy's Pacific Missile Range Facility.

|**SOURCE: Courtesy of NASA, Dryden Flight Center**

55

Solar Cells: Photovoltaics

56

Chandrayaan-2 spacecraft

https://www.indiatoday.in/science/story/chandrayaan-2-spacecraft-launcher-lander-rover-orbiter-explained-1568806-2019-07-14

56

Solar Cells: Photovoltaics

57

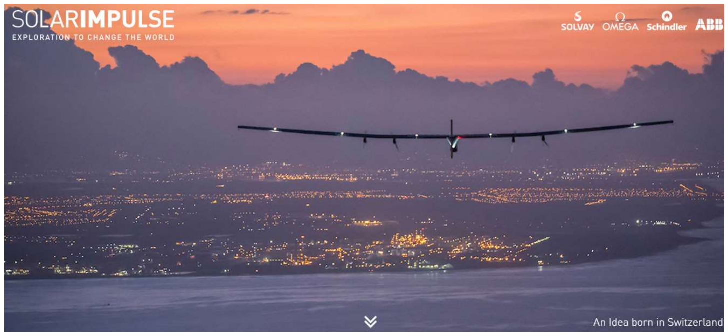

OUR ADVENTURE

In 2015 started the attempt of the First Round-The-World Solar Flight, from Abu Dhabi to Hawaii, already achieving the longest solo solar flight ever achieved in aviation history.

Bertrand Piccard and André Borschberg, our two Pilots and Founders, will continue to fly around the world with no fuel in 2016, rising up to technical, human and operational challenges that have never been faced before.

57

58

« Imagine energy reserves increasing during flight! To make this dream a reality, we had to make maximum use of every single watt supplied by the sun, and store it in our batteries. We tracked down every possible source of energy efficiency. »

André Borschberg

58

59

Solar cell inventors at Bell Labs (left to right) Gerald Pearson, Daryl Chapin and Calvin Fuller are checking a Si solar cell sample for the amount of voltage produced (1954).

SOURCE: Courtesy of Bell Labs, Lucent Technologies

59

60

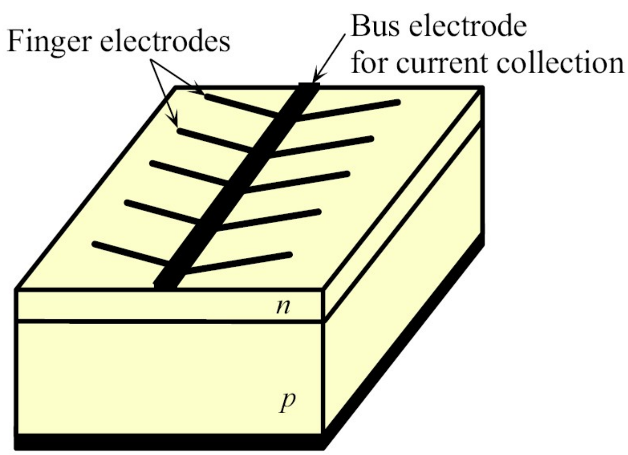

Finger electrodes on the surface of a solar cell reduce the series resistance.

60

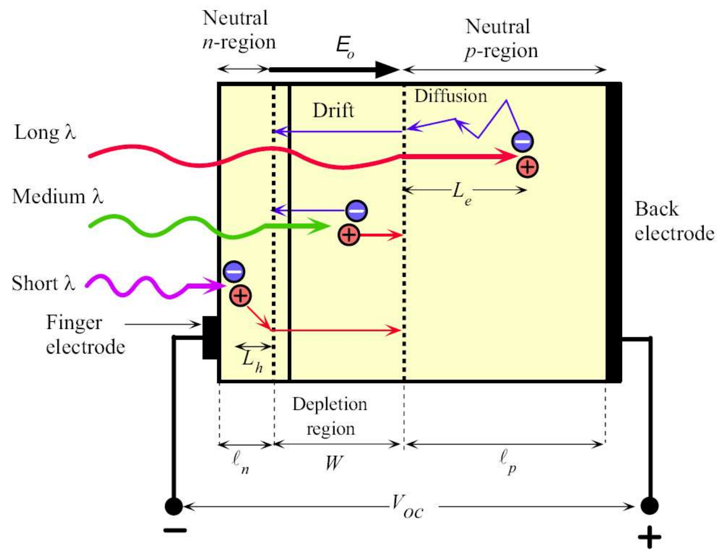

The principle of operation of the solar cell (exaggerated features to highlight principles)

61

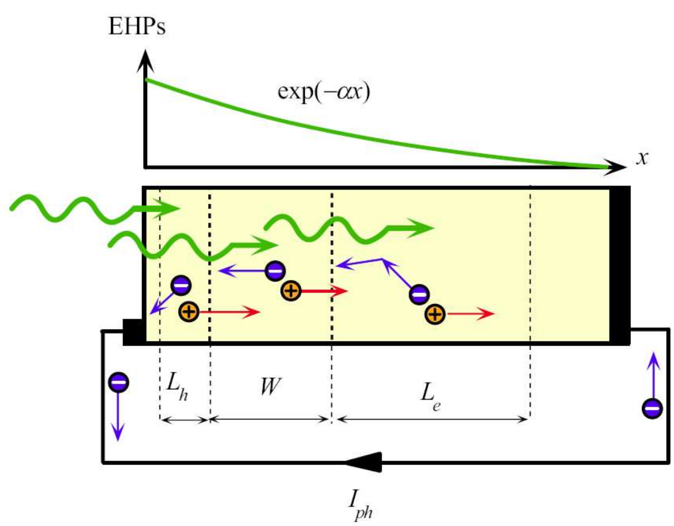

Photogenerated carriers within the volume $L_h + W + L_e$ give rise to a photocurrent I_{ph}. The variation in the photegenerated EHP concentration with distance is also shown where a is the absorption coefficient at the wavelength of interest.

62

Solar Spectra

63

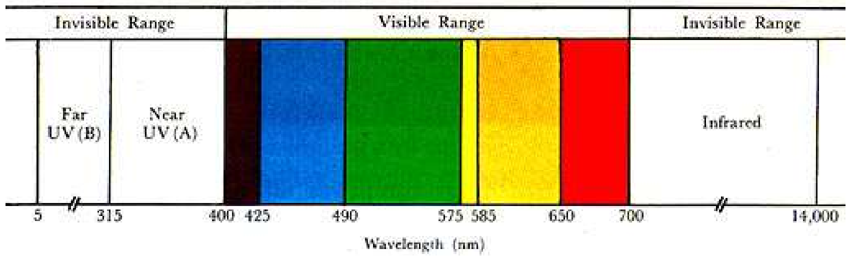

63

Solar Cells

64

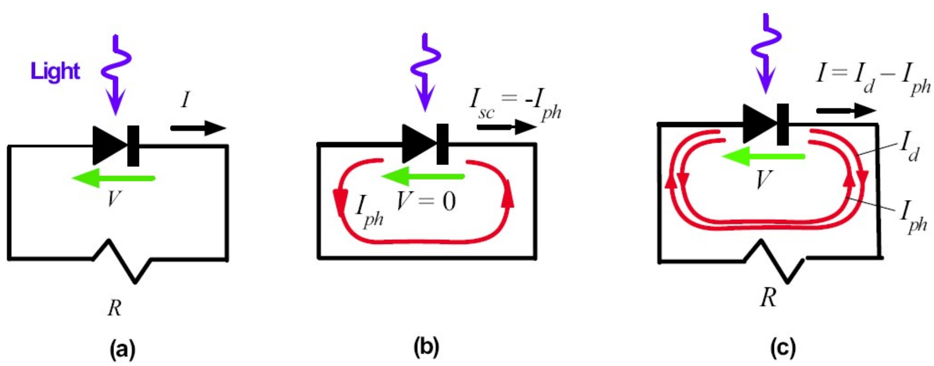

(a) The solar cell connected to an external load R and the convention for the definitions of positive voltage and positive current.
(b) The solar cell in short circuit. The current is the photocurrent, I_{ph}.
(c) The solar cell driving an external load R. There is a voltage V and current I in the circuit.

64

65

Solar Cells

Short circuit solar cell current in light

$$I_{\mathrm{sc}} = -I_{\mathrm{ph}} = -KI$$

Photocurrent generated by light

Light intensity

Constant that depends on the particular device

Solar cell *I-V*

$$I = -I_{\mathrm{ph}} + I_o\left[\exp\left(\frac{eV}{\eta kT}\right) - 1\right]$$

where I_o is the reverse saturation current and η is the ideality factor: 1 - 2

65

66

Solar Cells: I-V Characteristics

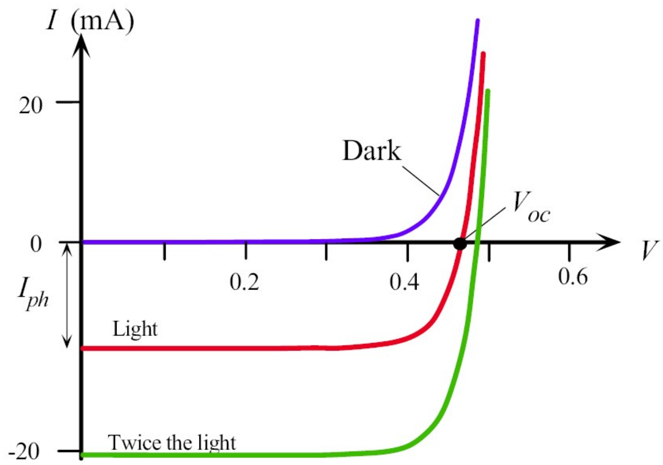

Typical *I-V* characteristics of a Si solar cell. The short circuit current is I_{ph} and the open circuit voltage is V_{OC}. The *I-V* curves for positive current requires an external bias voltage. Photovoltaic operation is always in the negative current region.

66

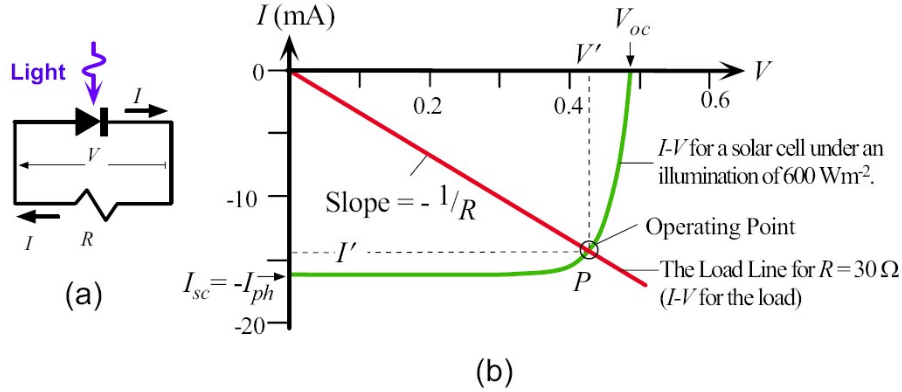

(a) When a solar cell drives a load *R*. *R* has the same voltage as the solar cell but the current through it is in the opposite direction to the convention that current flows from high to low potential. (b) The current *I*′ and voltage *V*′ in the circuit of (a) can be found from a load line construction. Point *P* is the operating point (*I*′, *V*′). The load line is for *R* = 30 Ω.

67

Solar Cells

The load line

$$I = -\frac{V}{R}$$

The actual current *I*′ and voltage *V*′ in the circuit must satisfy both the *I* - *V* characteristics of the solar cell and the load.

Definition of fill factor

$$\mathrm{FF} = \frac{I_m V_m}{I_{\mathrm{sc}} V_{\mathrm{oc}}}$$

The FF is a measure of the closeness of the solar cell *I-V* curve to the rectangular shape (the ideal shape).

68

69

Solar Cells

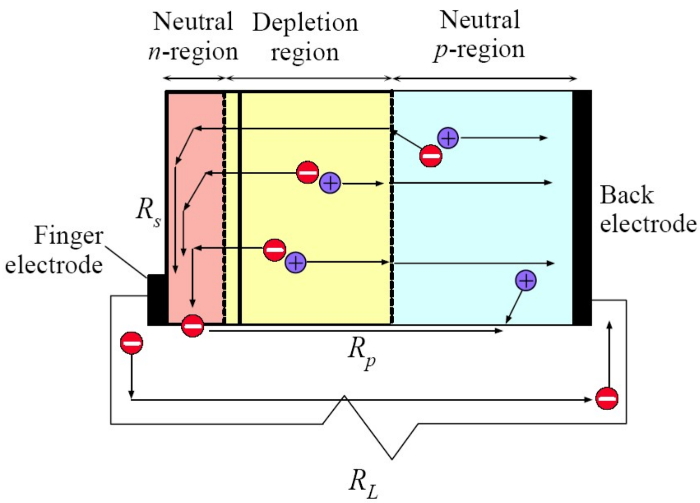

Series and shunt resistances and various fates of photogenerated EHPs.

69

70

Solar Cells

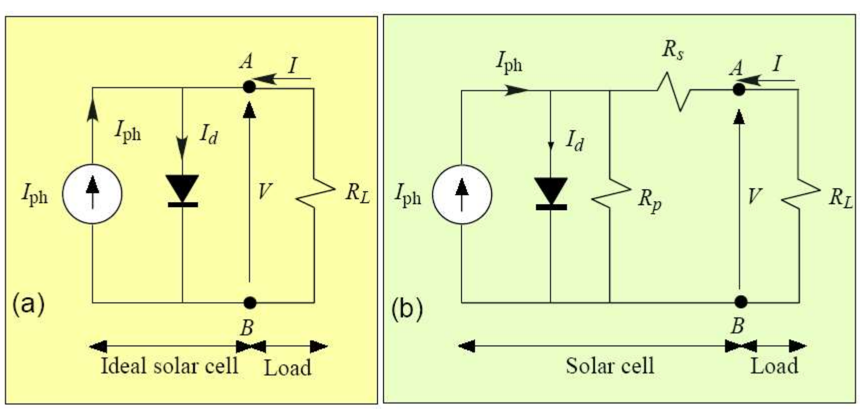

The equivalent circuit of a solar cell
(a) Ideal pn junction solar cell
(b) Parallel and series resistances R_s and R_p.

70

Solar Cells

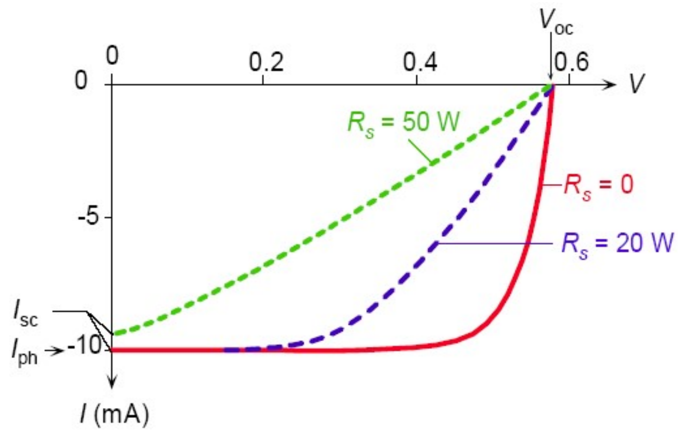

The series resistance broadens the I–V curve and reduces the maximum available power and hence the overall efficiency of the solar cell. The example is a Si solar cell with $\eta \approx 1.5$ and $I_o \approx 3 \times 10^{-6}$ mA. Illumination is such that the photocurrent $I_{ph} = 10$ mA.

71

Solar Cells: Designs

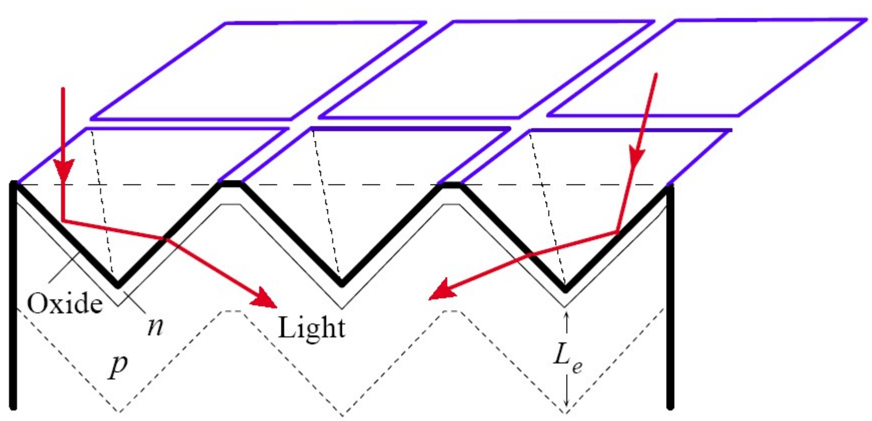

Inverted pyramid textured surface substantially reduces reflection losses and increases absorption probability in the device.

72

Solar Cells: Designs

Table 6.3 Typical characteristics of various solar cells at room temperature under AM1.5 illumination of 1000 W m^{-2}

Semiconductor	E_g (eV)	V_{oc} (V)	J_{sc} (mA cm^{-2})	FF	η (%)	Comments
Si, single crystal	1.1	0.5–0.7	42	0.7–0.8	16–24	Single crystal, PERL
Si, polycrystalline	1.1	0.5–0.65	38	0.7–0.8	12–19	
Amorphous Si:Ge:H film					8–13	Amorphous film with tandem structure, convenient large-area fabrication
GaAs, single crystal	1.42	1.02	28	0.85	24–25	
GaAlAs/GaAs, tandem		1.03	27.9	0.864	24.8	Different bandgap materials in tandem increases absorption efficiency
GaInP/GaAs, tandem		2.5	14	0.86	25–30	Different bandgap materials in tandem increases absorption efficiency
CdTe, thin film	1.5	0.84	26	0.75	15–16	
InP, single crystal	1.34	0.87	29	0.85	21–22	
$CuInSe_2$	1.0				12–13	

NOTE: AM1.5 refers to a solar illumination of "Air Mass 1.5," which represents solar radiation falling on the Earth's surface with a total intensity (or irradiance) of 1000 W m^{-2}. AM1.5 is widely used for comparing solar cells.

73

Solar Cells: Designs

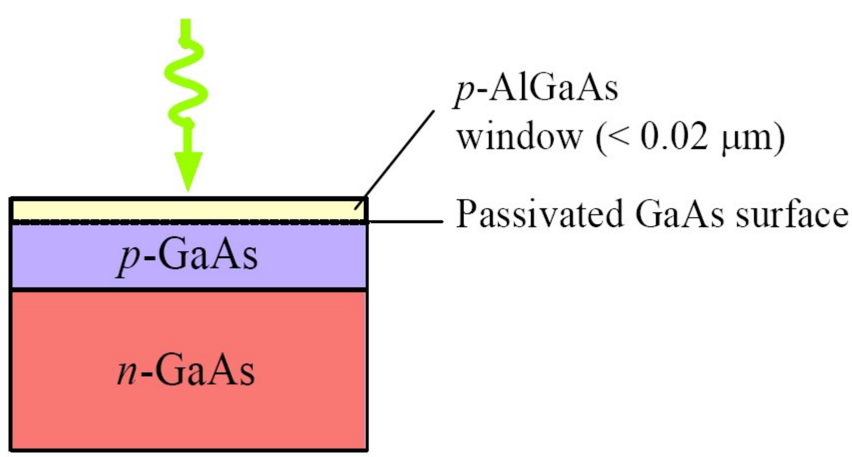

AlGaAs window layer on GaAs passivates the surface states and thereby increases the photogeneration efficiency.

74

Solar Cells: Designs

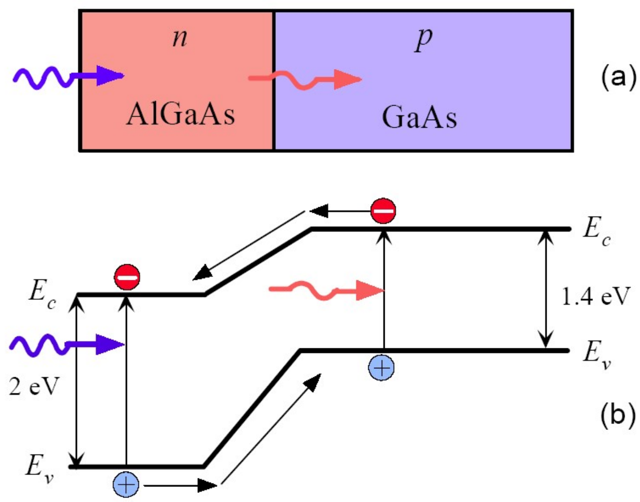

A heterojunction solar cell between two different bandgap semiconductors (GaAs and AlGaAs)

75

Solar Cells: Designs

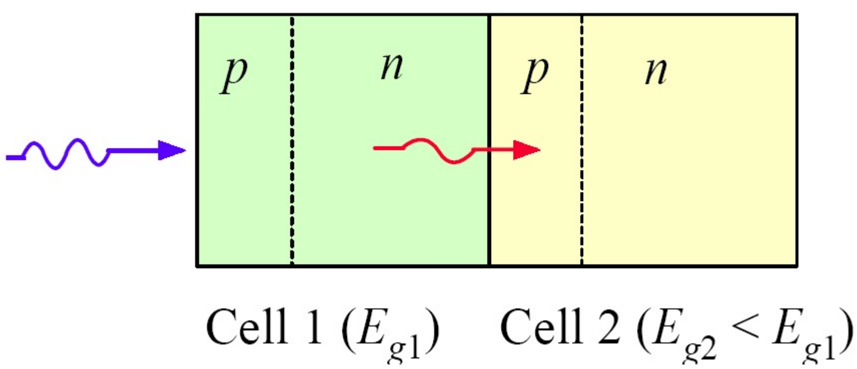

A tandem cell. Cell 1 has a wider bandgap and absorbs energetic photons with $h\nu > E_{g1}$. Cell 2 absorbs photons that pass cell 1 and have $h\nu > E_{g2}$.

76